EPJ Draft 1.0

Nuclear Polarization of Molecular Hydrogen Recombined on a Silicon-based Polymer Surface

The HERMES Collaboration

A. Airapetian,[30] N. Akopov,[30] Z. Akopov,[30] M. Amarian,[6,30] V.V. Ammosov,[22] A. Andrus,[15] E.C. Aschenauer,[6] W. Augustyniak,[29] R. Avakian,[30] A. Avetissian,[30] E. Avetissian,[10] P. Bailey,[15] V. Baturin,[21] C. Baumgarten, [19] M. Beckmann,[5] S. Belostotski,[21] S. Bernreuther,[8] N. Bianchi,[10] H.P. Blok,[20,28] H. Böttcher,[6] A. Borissov,[17] A. Borysenko,[10] M. Bouwhuis,[15] J. Brack,[4] A. Brüll,[16] V. Bryzgalov,[22] G.P. Capitani,[10] H.C. Chiang,[15] G. Ciullo,[9] M. Contalbrigo,[9] G. Court,[32] P.F. Dalpiaz,[9] R. De Leo,[3] L. De Nardo,[1] E. De Sanctis,[10] E. Devitsin,[18] P. Di Nezza,[10] M. Düren,[13] M. Ehrenfried,[8] A. Elalaoui-Moulay,[2] G. Elbakian,[30] F. Ellinghaus,[6] U. Elschenbroich,[12] J. Ely,[4] R. Fabbri,[9] A. Fantoni,[10] A. Fechtchenko,[7] L. Felawka,[26] B. Fox,[4] J. Franz,[11] S. Frullani,[24] G. Gapienko,[22] V. Gapienko,[22] F. Garibaldi,[24] K. Garrow,[1,25] E. Garutti,[20] D. Gaskell,[4] G. Gavrilov,[5,26] V. Gharibyan,[30] G. Graw,[19] O. Grebeniouk,[21] L.G. Greeniaus,[1,26] I. Gregor,[6] W. Haeberli,[31] K. Hafidi,[2] M. Hartig,[26] D. Hasch,[10] D. Heesbeen,[20] M. Henoch,[8] R. Hertenberger,[19] W.H.A. Hesselink,[20,28] A. Hillenbrand,[8] M. Hoek,[13] Y. Holler,[5] B. Hommez,[12] G. Iarygin,[7] A. Ivanilov,[22] A. Izotov,[21] H.E. Jackson,[2] A. Jgoun,[21] R. Kaiser,[14] E. Kinney,[4] A. Kisselev,[21] H. Kolster, [19,28] K. Königsmann,[11] M. Kopytin,[6] V. Korotkov,[6] V. Kozlov,[18] B. Krauss,[8] V.G. Krivokhijine,[7] L. Lagamba,[3] L. Lapikás,[20] A. Laziev,[20,28] P. Lenisa,[9] P. Liebing,[6] L.A. Linden-Levy,[15] K. Lipka,[6] W. Lorenzon,[17] J. Lu,[26] B. Maiheu,[12] N.C.R. Makins,[15] B. Marianski,[29] H. Marukyan,[30] F. Masoli,[9] V. Mexner,[20] N. Meyners,[5] O. Mikloukho,[21] C.A. Miller,[1,26] Y. Miyachi,[27] V. Muccifora,[10] A. Nagaitsev,[7] E. Nappi,[3] Y. Naryshkin,[21] A. Nass,[8] M. Negodaev,[6] W.-D. Nowak,[6] K. Oganessyan,[5,10] H. Ohsuga,[27] N. Pickert,[8] S. Potashov,[18] D.H. Potterveld,[2] M. Raithel,[8] D. Reggiani,[9] P.E. Reimer,[2] A. Reischl,[20] A.R. Reolon,[10] C. Riedl,[8] K. Rith,[8] G. Rosner,[14] A. Rostomyan,[30] L. Rubacek,[13] J. Rubin,[15] D. Ryckbosch,[12] Y. Salomatin,[22] I. Sanjiev,[2,21] I. Savin,[7] C. Scarlett,[17] A. Schäfer,[23] C. Schill,[11] G. Schnell,[6] K.P. Schüler,[5] A. Schwind,[6] J. Seele,[15] R. Seidl,[8] B. Seitz,[13] R. Shanidze,[8] C. Shearer,[14] T.-A. Shibata,[27] V. Shutov,[7] M.C. Simani,[20,28] K. Sinram,[5] M. Stancari,[9] M. Statera,[9] E. Steffens,[8] J.J.M. Steijger,[20] H. Stenzel,[13] J. Stewart,[6] U. Stösslein,[4] P. Tait,[8] H. Tanaka,[27] S. Taroian,[30] B. Tchuiko,[22] A. Terkulov,[18] A. Tkabladze,[12] A. Trzcinski,[29] M. Tytgat,[12] A. Vandenbroucke,[12] P. van der Nat,[20,28] G. van der Steenhoven,[20] M.C. Vetterli,[25,26] V. Vikhrov,[21] M.G.

Vincter,[1] C. Vogel,[8] M. Vogt,[8] J. Volmer,[6] C. Weiskopf,[8] J. Wendland,[25,26] J. Wilbert,[8] T. Wise,[31] G. Ybeles Smit,[28] S. Yen,[26] B. Zihlmann,[20] H. Zohrabian,[30] P. Zupranski[29]

[1]Department of Physics, University of Alberta, Edmonton, Alberta T6G 2J1, Canada

[2]Physics Division, Argonne National Laboratory, Argonne, Illinois 60439-4843, USA

[3]Istituto Nazionale di Fisica Nucleare, Sezione di Bari, 70124 Bari, Italy

[4]Nuclear Physics Laboratory, University of Colorado, Boulder, Colorado 80309-0446, USA

[5]DESY, Deutsches Elektronen-Synchrotron, 22603 Hamburg, Germany

[6]DESY Zeuthen, 15738 Zeuthen, Germany

[7]Joint Institute for Nuclear Research, 141980 Dubna, Russia

[8]Physikalisches Institut, Universität Erlangen-Nürnberg, 91058 Erlangen, Germany

[9]Istituto Nazionale di Fisica Nucleare, Sezione di Ferrara and Dipartimento di Fisica, Università di Ferrara, 44100 Ferrara, Italy

[10]Istituto Nazionale di Fisica Nucleare, Laboratori Nazionali di Frascati, 00044 Frascati, Italy

[11]Fakultät für Physik, Universität Freiburg, 79104 Freiburg, Germany

[12]Department of Subatomic and Radiation Physics, University of Gent, 9000 Gent, Belgium

[13]Physikalisches Institut, Universität Gießen, 35392 Gießen, Germany

[14]Department of Physics and Astronomy, University of Glasgow, Glasgow G12 8QQ, United Kingdom

[15]Department of Physics, University of Illinois, Urbana, Illinois 61801-3080, USA

[16]Laboratory for Nuclear Science, Massachusetts Institute of Technology, Cambridge, Massachusetts 02139, USA

[17]Randall Laboratory of Physics, University of Michigan, Ann Arbor, Michigan 48109-1120, USA

[18]Lebedev Physical Institute, 117924 Moscow, Russia

[19]Sektion Physik, Universität München, 85748 Garching, Germany

[20]Nationaal Instituut voor Kernfysica en Hoge-Energiefysica (NIKHEF), 1009 DB Amsterdam, The Netherlands

[21]Petersburg Nuclear Physics Institute, St. Petersburg, Gatchina, 188350 Russia

[22]Institute for High Energy Physics, Protvino, Moscow oblast, 142284 Russia

[23]Institut für Theoretische Physik, Universität Regensburg, 93040 Regensburg, Germany

[24]Istituto Nazionale di Fisica Nucleare, Sezione Roma 1, Gruppo Sanità and Physics Laboratory, Istituto Superiore di Sanità, 00161 Roma, Italy

[25]Department of Physics, Simon Fraser University, Burnaby, British Columbia V5A 1S6, Canada

[26]TRIUMF, Vancouver, British Columbia V6T 2A3, Canada

[27]Department of Physics, Tokyo Institute of Technology, Tokyo 152, Japan

[28]Department of Physics and Astronomy, Vrije Universiteit, 1081 HV Amsterdam, The Netherlands

[29]Andrzej Soltan Institute for Nuclear Studies, 00-689 Warsaw, Poland

[30]Yerevan Physics Institute, 375036 Yerevan, Armenia

[31]Department of Physics, University of Wisconsin-Madison, Madison, Wisconsin 53706 USA

[32]Physics Department, University of Liverpool, Liverpool L69 7ZE, United Kingdom

Received: May 16, 2003/ Revised version:

Abstract. The nuclear polarization of H_2 molecules formed by recombination of polarized H atoms on surface of a storage cell coated with a silicon-based polymer has been measured by using the longitudinal double spin asymmetry in deep inelastic positron-proton scattering. The measurement has evidenced that the recombining atoms emanating from the surface present a significant nuclear polarization.

PACS. 29.25.P Polarized Targets – 34.09.+q Atomic and Molecular Collision Processes and Interactions – 39.10.+j Atomic and Molecular Beams Sources and Techniques – 13.88.+e Polarization in Interactions and Scattering

1 Introduction

During the past years, increased use has been made of polarized hydrogen and deuterium gas targets, which are placed in the circulating beams of storage rings. In order to increase their thickness over that obtained by a jet of polarized atoms, the beam from atomic sources is directed into an open, cooled cell (*storage cell*) in which the atoms make several hundred collisions before escaping. In order to maintain high polarization, the storage cells are usually coated with organosilicon, chemicallly nonreactive materials [1–3]. These targets offer distinct advantages: they present no dilution of the polarization, they enable the detection of low-energy recoils, they guarantee high-systematic precision thanks to the rapid switching of the sign of the polarization and the gas itself does not suffer radiation damage bacause it is continously replenished. Examples of the successful use of this technique are measurements of spin correlation parameters in proton-proton scattering at the Indiana University Cyclotron Facility (IUCF) [4] and studies of electromagnetic form factors at the storage rings VEPP-3 in Novosibirsk [5] and AmPS at NIKHEF, Amsterdam [6]. The HERMES experiment uses such an internal target to study deep inelastic scattering of positrons off polarized H nuclei [7, 8]. The precise knowledge of the polarization value is required to measure the spin-dependent processes. Unlike experiments with hadron beams or with medium-energy electron beams, at HERMES energies there is no scattering process which could provide the absolute value of the target polarization with acceptable statistics. Therefore,

for the HERMES experiment a target polarimeter with good absolute precision is required [9]. While the polarization of the atoms is measured directly, the polarization of H_2 molecules derived from recombination in the target cell is unknown; this causes an additional systematic uncertainty in the target polarization. The nuclear polarization of recombined H_2 molecules has been recently studied in a separate experiment [10]: polarized atoms have been made to recombine using a copper surface and the nuclear polarization of the molecules has been measured by elastic proton-proton scattering. The result of this measurement is not applicable to the silicon-polymer coated storage cells where surface characteristics different from those of a metal are involved. The other existing measurement of polarization of recombined atoms concerns tensor polarized D atoms and was also observed on a copper surface [11]. The present work reports the first measurement of the polarization of molecules which have been obtained via recombination of polarized atoms on a silicon-based polymer. The measurement has been performed by detecting a well known spin correlation parameter in the deep inelastic scattering of polarized leptons off a polarized target [12]: the spectrometer of the HERMES experiment has been employed for this purpose. A signficant spin polarization has been measured which can be traced back to a long-lived nuclear polarization of atoms chemisorbed to the insulating surface. The results of the present recombination studies are reported in Fig.1. The parameter $\beta = P_m/P_a$ expresses the ratio between the nuclear polarization of molecules after recombination (P_m) and atoms before recombination (P_a).

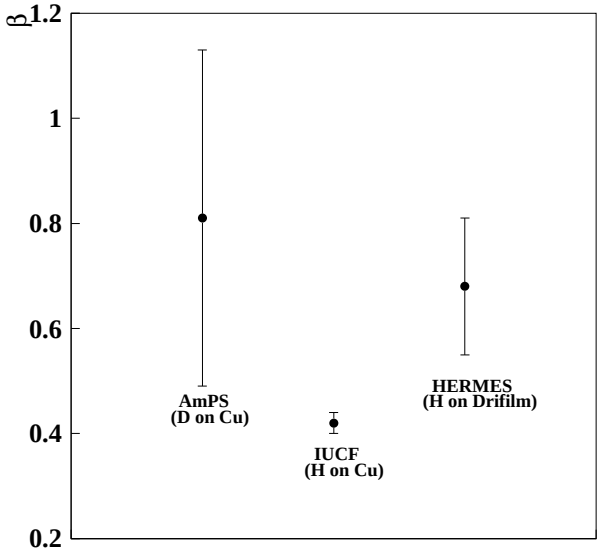

Fig. 1. Summary of the existing recombination studies. The newly obtained HERMES meaurement at 260 K with a holding field of 330 mT, is compared to the measurement by AmPS and IUCF obtained at room temperature and magnetic holding fields of 28 mT and 440 mT respectively.

2 Experimental Setup

2.1 The HERMES Spectrometer

The HERMES experiment is installed in the HERA storage ring at the DESY laboratory in Hamburg. It uses the positron beam of 27.6 GeV energy with maximum current of 40 mA. The positrons become transversely polarized by emission of synchrotron radiation [13]. Longitudinal polarization of the positron beam at the interaction point is achieved by spin rotators situated upstream and down-

stream the experiment. The beam polarization is continuously measured using Compton back-scattering of circularly polarized light. Two polarimeters are used, one measuring the transverse polarization in the HERA West straight section [14] and the other measuring the longitudinal polarization near the HERMES target [15] with low systematic uncertainties. Positron identification in the momentum range 2.1 to 27.6 GeV is accomplished by using a lead-glass block calorimeter, a transition-radiation detector and a preshower hodoscope. This system provides positron identification with an average efficiency higher than 98 % and a negligible hadron contamination. The luminosity is measured by detecting Bhabha scattered target electrons in coincidence with the scattered positrons in a pair of electromagnetic calorimeters [16]. The HERMES spectrometer is described in detail in [17].

2.2 The Hydrogen Target

A schematic diagram of the HERMES target is shown in Fig. 2. A beam of polarized hydrogen atoms is generated by an atomic beam source (ABS) [18] and injected into the center of the storage cell [19] via a side tube. The atoms then diffuse to the open ends of the cell where they are removed by a high speed pumping system. The cell has been coated with *Drifilm*, a silicon-based polymer providing radiation hardness properties, as demanded in the accelerator environment [20]. The coating procedure which has been adopted is described in detail in Ref. [3]. The storage cell is protected by a system of tungsten collimators upstream of the target from the intense synchrotron

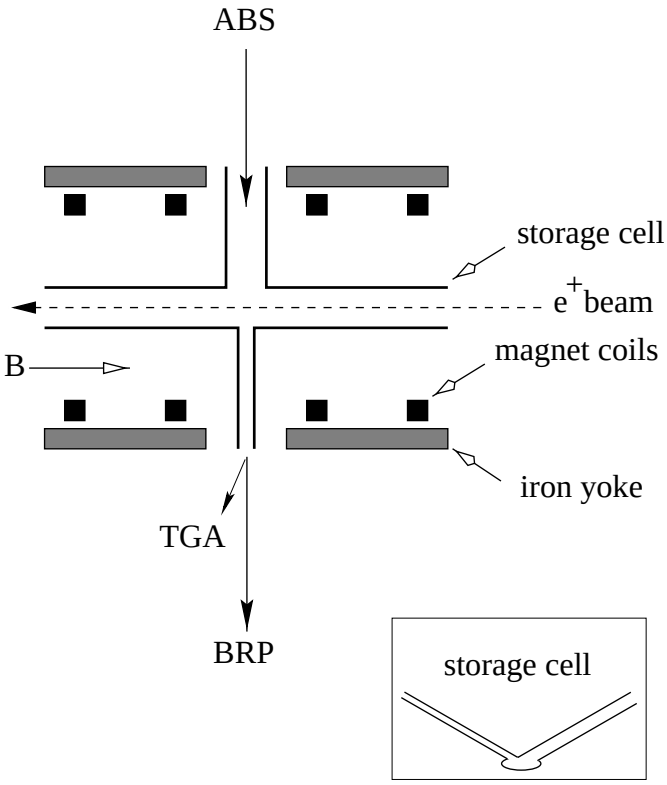

Fig. 2. A schematic layout of the HERMES hydrogen target. From top to bottom: injection tube for atomic beam source (ABS) [18], target chamber with cell and magnet, sample tube and directions of target gas analyzer (TGA) and Breit-Rabi polarimeter (BRP). The inset shows the cross section of the storage cell with injection (right) and sample (left) tubes.

radiation emerging from the machine magnets. The exact dose at the cell surface is not known. It is routinely observed that the original hydrofobic Drifilm surfaces turn into hydrophil ones after exposure to the 27.5 GeV electron beam as indicated by their different wetting properties. A magnetic field of 330 mT sorrounding the cell provides a quantization axis for the spins and inhibits nuclear spin relaxation by effectively decoupling nucleon and electron spins. The beam emerging from a second side tube of the cell is analyzed by a Breit-Rabi polarimeter (BRP) [9]

to measure the polarization of the atoms and a target gas analyzer (TGA) [21] to determine the atomic fraction.

2.2.1 The target polarization

The average target polarization as seen by the positron beam is described by the following expression [22]:

$$P_T = \alpha_0 \alpha_r P_a + \alpha_0 (1 - \alpha_r) \beta P_a \tag{1}$$

In Eq.1 P_a is the nuclear polarization of the atoms in the cell. The parameter $\beta = P_m/P_a$ represents the relative polarization of the recombined molecules with respect to the atomic polarization before recombination ($0 \leq \beta \leq 1$), and it is the subject of the measurement presented in this paper. The atomic fractions α_0 and α_r are defined below. Molecules inside the HERMES target have three origins: residual gas in the scattering chamber containing the storage cell, molecules ballistically injected by the ABS and atoms that recombine into molecules after entering the cell. Each contribution is directly measured with dedicated calibrations by the TGA as described in Ref. [21]. For the first two, the nucleons are not polarized while the recombined molecules may have a remnant nuclear polarization. The atomic fraction is defined as:

$$\alpha = \frac{n_a}{n_a + 2n_m} \tag{2}$$

where n_a and n_m are the atomic and molecular populations averaged over the cell, is factorized into two terms α_0 and α_r. α_0 is fraction of the target in atomic form for the ideal case of no recombination inside the cell (α_r =1). In nearly every case, however, recombination does occur on the cell walls and α_r, the fraction of the atoms that do not recombine, is < 1. As the particles sampled from the center of the cell have experienced a different average number of wall collisions than the ones at the edges of the cell, the properties of the sample beam are slightly different from the average values in the cell. In order to relate the average values over the cell (α_r and P_a) to the corresponding measurements on the sample beam (α_r^{TGA} and P^{BRP}), so called *sampling corrections* have to be introduced. The sampling corrections depend on the sensitivity of the BRP and the TGA to the different parts of the cell and are derived by Monte-Carlo simulations of the molecular flow by tracking the history of gas particles traveling through the storage cell as described in Ref. [23].

3 Measurement

3.1 Method

The method adopted to extract the relative molecular polarization β makes use of the double spin asymmetry in the deep inelastic scattering of a longitudinally polarized positron beam off a longitudinally polarized proton target. The cross sections σ^+ and σ^- for parallel and antiparallel orientation of beam and target polarizations respectively, are related to the unpolarized cross section σ_0 by:

$$\sigma^{+/-} = \sigma_0 (1 \mp P_B P_T A_{||}) \tag{3}$$

where P_B and P_T are the beam and target polarizations and $A_{||}$ is the longitudinal spin-correlation coefficient. In

the experiment, the count rate asymmetry is measured:

$$C_{||} = \frac{(N/L)^- - (N/L)^+}{(N/L)^- + (N/L)^+} = P_B P_T A_{||} \quad (4)$$

where 4 $N^{+,-}$ denotes the number of events with parallel (anti-parallel) beam and target spins orientations corrected for the background arising from charge symmetric processes, as γ conversion, and L is the corresponding luminosity. Two measurements have been performed to determine the polarization of the molecules. one with (almost) pure atomic target of known polarization and a second with enhanced recombination. The increase in the recombination rate was achieved by increasing the temperature of the target cell from 100 K (normal running conditions) to 260 K. In this temperature range the main mechanism responsible for recombination in the target cell is the Eley-Rideal mechanism [24] in which an atom in the gas phase hits a chemically bound atom on the surface with enough kinetic energy to overcome the activation barrier. The increase in the target temperature results in an increase of the kinetic energy of the atoms in the volume and in a higher recombination probability [25]. The target parameters for the two different temperatures are reported in Table 1: a large increase in the fraction $(1-\alpha_r)$ of recombined atoms from 0.055 at 100 K to 0.74 at 260 K can be deduced. As the spin-correlation coefficient $A_{||}$ is independent from the experimental conditions, we can write:

$$(\frac{C_{||}}{P_T P_B})^{100K} = (\frac{C_{||}}{P_T P_B})^{260K} \quad (5)$$

The target polarizations can be expressed by (see Eq. (1)):

$$P_T^{100K} = \alpha_0^{100K}[\alpha_r^{100K} + (1-\alpha_r^{100K})\beta^{100K}]P_a^{100K} \quad (6)$$

Table 1. Atomic polarization and atomic fraction at 100 K and 260 K [22]

T_{cell}	P_a	α_0	α_r
100 K	0.906 ± 0.01	0.96 ± 0.03	0.945 ± 0.035
260 K	0.939 ± 0.015	0.96 ± 0.03	0.26 ± 0.04

$$P_T^{260K} = \alpha_0^{260K}[\alpha_r^{260K} + (1-\alpha_r^{260K})\beta^{260K}]P_a^{260K} \quad (7)$$

The values for $\alpha_0^{100K,260K}, \alpha_r^{100K,260K}, P_a^{100K,260K}$ are reported in Table 1.

3.2 Extraction of the parameter β

In order to compare the asymmetries of Eq. 5, a minimization procedure has been used. Eq. 5 has two unknowns: β^{100K} and β^{260K}, which have been considered independent since the surface conditions at 100 K and 260 K might be different. In Eq. 5 two unknowns are present: β^{100K} and β^{260K}, as the surface conditions at 100 K and 260 K might be different, they have been considered independently. The value β^{260K} has been determined by varying its value until the function $F(\beta)$ described by:

$$F(\beta) = \sum_{bins} \left[\frac{(\frac{C_{||i}}{P_B P_T})^{260K} - (\frac{C_{||i}}{P_B P_T})^{100K}}{\left((\delta_{C||i}^{260K})^2 + (\delta_{C||i}^{100K})^2\right)^{1/2}} \right]^2 \quad (8)$$

was minimized. The minimization has been studied as a function of the parameter β^{100K}. In Eq.8 $C_{||i}$ is the count rate asymmetry in the i-bin of the kinematic plane and $\delta_{C||i}$ is its related statistical uncertainty (the statistical uncertainties of P_T and P_B are negligible). The summation is made over all the kinematic bins of the asymmetry measurement. The binning of the kinematic plane has been accomplished according to the one adopted in the

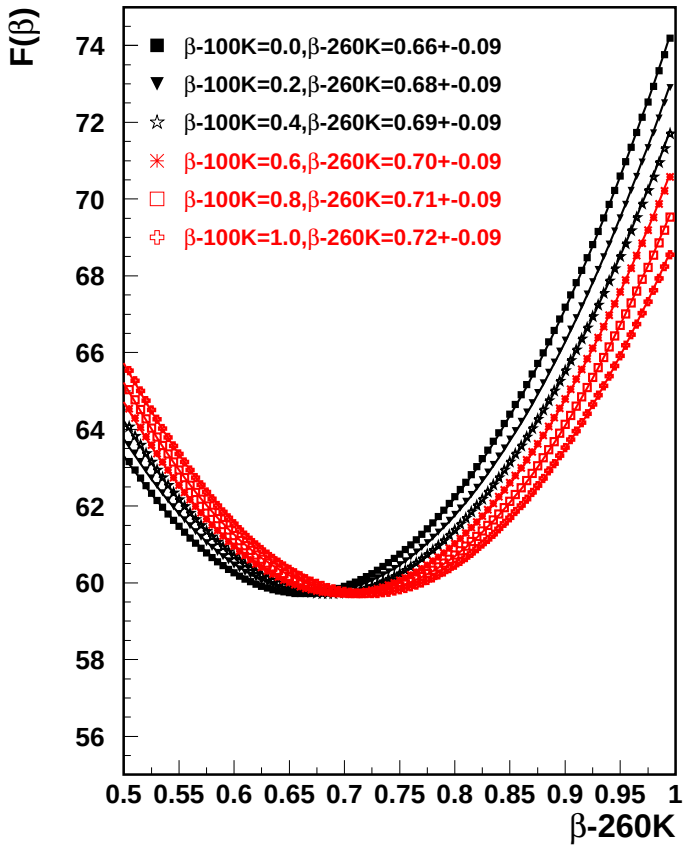

Fig. 3. $F(\beta)$ as a function of β^{260K} for fixed values of β^{100K} in the allowed range $0 \leq \beta^{100K} \leq 1$.

extraction of the g_1^p spin-dependent structure function of the proton from the $A_{||}$ asymmetry, as it is described in [12]. The result of the minimization procedure is shown in Fig. 3

As at 100 K only a few percent of the gas is in molecular form (0.055 ± 0.035, see Table 1), the final result is practically insensitive to the value assumed for β^{100K}. Using the extreme assumption $\beta^{100K} = 0.5 \pm 0.5$, the following value has been obtained for β^{260K}:

$$\beta^{260K} = 0.68 \pm 0.09_{stat} \pm 0.06_{syst} \qquad (9)$$

The uncertainty of the measurement is dominated by the low statistics of the data taken at 260 K (0.19 million events) compared to the 100 K data sample (2.5 million events). The statistical error was calculated by highering the minimum of $F(\beta^{260K})$ by one unit and was found to be rather independent from the choice of β^{100K}. The main source of the systematic error arises from the uncertainty in α_r^{260K}. The rapid growth of the systematic error imposed by the sampling technique for values of α_r^{TGA} significantly below 1, as for the data taken at 260 K, excludes this method for the present study. In order to limit the uncertainty in α_r^{260K} an alternative method has been applied. Coincident Bhabha-scattering event rates detected by the luminosity monitor are proportional to the target density which, if the atomic flux injected in the cell is constant, depends on the atomic fraction. (The atoms recombined into molecules have a $\sqrt{2}$ higher density due to their lower velocity). The comparison of the Bhabha-rates detected at 100 K and 260 K allowed to limit the interval of α_r^{260K} as determined by the sampling method ($0.19 \leq \alpha_r^{260K} \leq 0.72$) to the more precise value reported in Table 1. The details of this measurement are given in [22]. Systematic uncertainties as the uncertainty in α_0 and P_B, which are common to both the 100 K and the 260 K measurements, cancel in the ratio in Eq.8. The stability of the result has been investigated by varying target data quality criteria and by varying the number of kinematic bins considered in Eq. 8: no systematic effect could be detected beyond the statistical accuracy.

3.3 Nuclear polarization of surface atoms

By assuming that the nucleon spins are not affected by the recombination process, the nuclear polarization of the molecule at its formation (P_m^0) can be evaluated by taking the average value of the polarization of the atom coming from the volume (P_a) and of the one sitting on the surface (P_s):

$$P_m^0 = \frac{P_a + P_s}{2} \tag{10}$$

The loss of polarization of the molecule after recombination has been well described in [10]. In free flight, the internal molecular fields B_c from the spin-rotation interaction and the direct dipole-dipole interaction cause the nuclei to rapidly precess around a direction which is skew to the external field by B_c/B. The orientation of B_c is randomized at each wall collision. Between successive wall collisions, the component of the polarization along the external field decreases by an amount $(B_c/B)^2$ and after n wall bounces:

$$P_m = P_m^0 e^{-n(B_c/B)^2} \tag{11}$$

where B_c for H_2 is 6.1 mT. For the HERMES cell, we have the values: $n \approx 300$ [23], $B \approx 330$ mT so that Eq. 11 allows one to conclude $P_m \approx 0.9 P_m^0$. From the extracted value of β^{260K} and making use of Eq. 10 and of the value for P_a^{260K} (see Table 1), we are able to give an estimate for the residual polarization of the atoms on the surface:

$$P_s^{260K} = 0.46 \pm 0.22_{tot}. \tag{12}$$

This evidences a residual nuclear polarization for the chemically bound surface atoms which recombine.

4 Discussion and Outlook

The present result differs from the one of the experiment described in Ref.[10] which indicated that residual atoms on a copper surface retain no polarizatoin at all. As both measurements are sensitive to the nuclear polarization of the molecular gas coming from the recombination process where one atom of each recombined molecule comes from the surface, they are actually comparing the nuclear spin relaxation time of atoms on the surface τ_r with the residence time on the surface τ_d. These times are related by the equation:

$$P_s = P_a \frac{\tau_r}{\tau_d + \tau_r} \tag{13}$$

By using the result of Eq. 12 and of Ref. [10] we can derive $\tau_r \approx \tau_d$ for *Drifilm* and $\tau_r \ll \tau_d$ for copper, evidencing that, as expected, for a metal surface the relaxation processes are much stronger than on an inert surface like silane.

An upper limit for the residence time of the atoms on the cell surface τ_d can be derived by considering a uniform surface where all the sites are catalytic and by using the equation:

$$\tau_d \approx \frac{N_s}{N_{inj}(1 - \alpha_r)} \tag{14}$$

where N_s is the total number of catalytic sites on the cell surface S, N_{inj} is the number of injected atoms per second. By assuming an area per surface site of $4\mathring{A}^2$, taking $S \approx 0.026 m^2$ [19], $N_{inj} \approx 6.5 \times 10^{16}$ atoms/s [18] and

$\alpha_r \approx 0.26$ (Tab. 1) one obtains $\tau_d \approx 14$ s and a relaxation time τ_r of the same order.

The result obtained for the Driflim showing a non-negligible polarization preserved by the surface atoms, is promising in view of the possible realization of a gaseous molecular target.

5 Conclusions

In summary, the longitudinal double spin asymmetry in deep-inelastic positron-proton scattering has been used to measure for the first time the nuclear polarization of the molecules produced by recombination of hydrogen atoms on a Drifilm coated storage cell. The measurement indicates that the atoms on the silane surface show significant nuclear polarization, different from the case of a metal surface where no residual polarization has been detected.

6 Acknowledgments

We gratefully acknowledge the DESY management for its support and the DESY stuff and the stuffs of the collaborating institutions. This work was supported by the FWO-Flanders, Belgium; the INTAS contribution from the European Commission; the European Commission IHP program under contract HPRN-CT-2000-00130; the German Bundesministerium für Bildung und Forschung (BMBF); the Italian Istituto Nazionale di Fisica Nucleare (INFN); Monbusho International Scientific Research Program, JSPS, and Toray Science Foundation of Japan; the Dutch Foundation for Fundamenteel Onderzoek der Materie (FOM); the U.K. Particle Physics and Astronomy Research Council and Engineering and Physical Sciences Research Council; and the U.S. Department of Energy and National Science Foundation.

References

1. G. E. Thomas et. al.; *Nucl.Instrum. and Meth. A* **257**, (1987), 32
2. D. R. Swenson and L.W. Anderson *Nucl. Instrum. and Meth. B* **29**, (1988), 627
3. J.A. Fedchak et al. *Nucl. Instrum. and Meth. A* **391**, (1997), 405
4. W.Haeberli et al., *Phys. Rev. C* **55**, (1997) 597,
5. R. Gilmann et al., *Phys. Rev. Lett.* **65**, (1990), 1733
6. M. Ferro-Luzzi et al., *Phys. Rev. Lett* **77**, (1996), 2630
7. HERMES Technical Design Report, DESY-PRC 93/06 (1993)
8. K. Rith *Progr. Part. Nucl. Phys* **49**, (2002), 245
9. C. Baumgarten et al. *Nucl. Instrum. and Meth. A* **482**, 606 (2002)
10. T. Wise et al. *Phys. Rev. Lett.* **87**, (2001), 042701
11. J. F. J. van den Brand et al. *Phys. Rev. Lett.* **78**, (1997), 1235
12. A. Airapetian et al.; *Phys. Lett. B* **442**, (1998), 484
13. A. A. Sokolov and I. M. Ternov, *Sov. Phys*, Doklady 8 (1964), 1203
14. D. P. Barber et al.; *Phys. Lett. B* **343** (1995), 436
15. M. Beckmann et al.; *Nucl. Instr. Meth. A* **479**, (2002) 334
16. Th. Benisch et al.; *Nucl. Instr. Meth. A* **471**, (2001) 314
17. Ackerstaff et al.; *Nucl. Instr. Meth. A* **417**, (1998), 230

18. A. Nass et al. *The HERMES polarized Atomic Beam Source*, to appear in Nucl. Instrum. and Meth. A

19. C. Baumgarten et al. *Nucl. Instrum. and Meth. A* **496**, 277 (2003)

20. R. Gilman et al. *Nucl. Instrum. and Meth. A* **327**, 277 (1993)

21. C. Baumgarten et al. *The gas analyzer of the target of the HERMES experiment*, to appear in *Nucl. Instrum. and Meth. A*

22. A. Airapetian et al. *Performance of the HERMES Hydrogen/Deuterium target* in preparation

23. C. Baumgarten et al. *Eur. Phys. J. D* **18**, (2002), 37

24. S. Holloway *Surf. Sci.***299/300**, (1994), 656

25. C. Baumgarten et al. *Nucl. Instrum. and Meth. A* **496**, 263 (2003)